

## A Mexacarbate Electrochemical Biosensor on Carbon Materials Based on a Functionalized Multiwalled Carbon Nanotube Modified Glassy Carbon Electrode

J. Tharini<sup>1,\*</sup>, Tse-Wei Chen<sup>2,3</sup>, Shen-Ming Chen<sup>2,\*</sup>, R. Saraswathi<sup>4</sup>,  
Mohamed S. Elshikh<sup>5</sup>, Noura M. Darwish<sup>6</sup>, Syang-Peng Rwei<sup>3,7</sup>

<sup>1</sup> Sethu Institute of Technology, Pulloor-626115, Kariapatti, TN, India

<sup>2</sup> Department of Chemical Engineering and Biotechnology, National Taipei University of Technology, Taipei 106, Taiwan.

<sup>3</sup> Research and Development Center for Smart Textile Technology, National Taipei University of Technology, Taipei 106, Taiwan, ROC

<sup>4</sup> Department of Materials Science, School of Chemistry, Madurai Kamaraj University, Madurai - 625 021, Tamilnadu, India

<sup>5</sup> Department of Botany and Microbiology, College of Science, King Saud University, P.O. Box 2455 Riyadh 11451, Saudi Arabia.

<sup>6</sup> Biochemistry Department, Ain Shams University, Cairo, Egypt.

<sup>7</sup> Institute of Organic and Polymeric Materials, National Taipei University of Technology, Taipei 106, Taiwan, ROC

\*E-mail: [smchen78@ms15.hinet.net](mailto:smchen78@ms15.hinet.net) (Shen-Ming Chen), [tharinichem@gmail.com](mailto:tharinichem@gmail.com) (J.Tharini)

Received: 15 April 2019 / Accepted: 18 June 2019 / Published: 30 June 2019

---

The commercial multi-walled carbon nanotube (MWCNT) was carboxylated using sulphuric and nitric acid and characterized by various techniques such as scanning electron spectroscopy, Infra-red spectroscopy and atomic force microscopy. The acid functionalized multiwalled carbon nanotube serves as the effective matrix for the sensing of carbamate pesticide namely mexacarbate. The electrochemical oxidation of mexacarbate at GCE and MWCNT/GCE follows heterogeneous electron transfer reaction. Different experimental parameters such as the effect of scan rate and pH were studied. Rotating disk electrode voltammetry studies confirm the one-electron transfer reaction. The sensor calibration plot for mexacarbamate was constructed by means of pulse technique. The acid functionalized multiwalled carbon nanotube sensor was applied to real water sample with the recovery percentage of 85-89%.

---

**Keywords:** Mexacarbate, differential pulse voltammetry, multi-walled carbon nanotube, glassy carbon electrode, calibration plot

## 1. INTRODUCTION

Carbamate pesticides are widely used as the insecticides due to their efficiency in producing a good crop yield [1,2]. The carbamate pesticides are *N*-substituted esters of carbamic acid with the structure  $R^1OCONHR^2$  where  $R^1$  is an aromatic or aliphatic group and  $R^2$  is a methyl or aromatic or benzimidazole group [3]. *N*-methyl carbamates form an important class of carbamate pesticides widely employed in agriculture [4]. Some of these commonly used carbamate pesticides are aldicarb, carbaryl, methiocarb, benomyl, methomyl, propoxur, and carbofuran. The lethal dosage of carbamate pesticides is in the range of 0.9 mg/kg to 8000 mg/kg depending on the pesticide. Aldicarb is denoted as the extremely hazardous pesticide with a lethal dosage of 0.9 mg/kg [5]. However, they are considered to be hazardous to human health, environment and, therefore, it is must to develop nanomaterials and methods for their rapid and sensitive determination of carbamate pesticides [6] Various methods such as solid phase extraction, supercritical fluid extraction, high-performance liquid chromatography coupled with mass spectrometric detection, gas chromatography and spectrophotometry have been applied in the detection of carbamate pesticides [7-12]. These conventional methods are sensitive and reliable but possess several disadvantages such as the need for expensive instrumentation, skilled technicians, time-consuming and not easily adaptable in field analysis. Alternatively, the electrochemical method offers a simple and inexpensive tool for the sensing of carbamate pesticides [13]. They are convenient, sensitive, selective and highly suitable for the fast monitoring of pesticides.

A survey of the literature reveals that only very few reports are available on the electrochemical detection of *N*-methylcarbamate pesticides [14-20] and to there have been only two reports on the electrochemical activity of aminocarb and mexacarbate at an unmodified glassy carbon electrode [16]. The oxidation of *N*-methylcarbamate occurs at high overpotential which can interfere with oxygen evolution reaction. For this reason, *N*-methylcarbamate is hydrolyzed to the corresponding phenol derivative which can be oxidized at relatively lower potential [14]. Conductive boron-doped diamond thin-film electrodes were used for the electrochemical detection of carbamate pesticides such as carbaryl, carbofuran, methyl 2-benzimidazole carbamate and bendiocarb [20]. Ni and others [15] applied chemometrics methods such as classical least square method, principal component regression and partial least squares for the simultaneous determination of propoxur, isoprocarb, carbofuran, and carbaryl. The voltammetric analysis of pesticides at chemically modified electrodes has been well documented [22, 23]. Several exclusive reviews on carbon nanotubes based electrochemical sensors, biosensors and energy storage devices have been published [24, 25].

In the present study, a differential voltammetry sensor has been developed for the detection of mexacarbate using the functionalized of carboxylated multi-walled carbon nanotubes of nanomaterials modified glassy carbon electrode (f-MWCNT/GCE). This is the first report on the use of multiwalled carbon nanotube as the chemically modified electrode for the electrochemical sensing of mexacarbate.

## 2. EXPERIMENTAL

### 2.1 Reagents and apparatus

Potassium dihydrogen phosphate, dipotassium hydrogen phosphate, acetic acid, sodium acetate, mexacarbate were purchased from Sigma–Aldrich. The stock solutions of mexacarbate (0.01M) were prepared by dissolving the appropriate quantity of the pesticide in 10 mL of acetonitrile. A known volume of the stock solution was diluted with the phosphate buffer solutions of respective pH to prepare the pesticide solution of desired concentration. Phosphate buffer solution (PBS) of 0.1 M concentration was prepared by mixing 0.1 M potassium dihydrogen phosphate(KHP) and 0.1 M dipotassium hydrogen phosphate( $\text{NaH}_2\text{PO}_4$ ).

### 2.2. Apparatus

Electrochemical measurements were performed on an electrochemical workstation (CH Instruments, USA, and Model 680). A one-compartment cell with provision for three electrodes comprising glassy carbon electrode (GCE,  $0.07 \text{ cm}^2$ ) as the working electrode, saturated calomel electrode (SCE) as the reference and large platinum foil electrode as the counter electrode. Surface morphological studies were carried out using high-resolution scanning electron microscope (HRSEM) (XL30-SFEG). The surface topography of the samples was obtained using an atomic force microscope (AFM) (Shimadzu 9500). The IR data were obtained using an FT-IR spectrometer (Shimadzu 8400S).

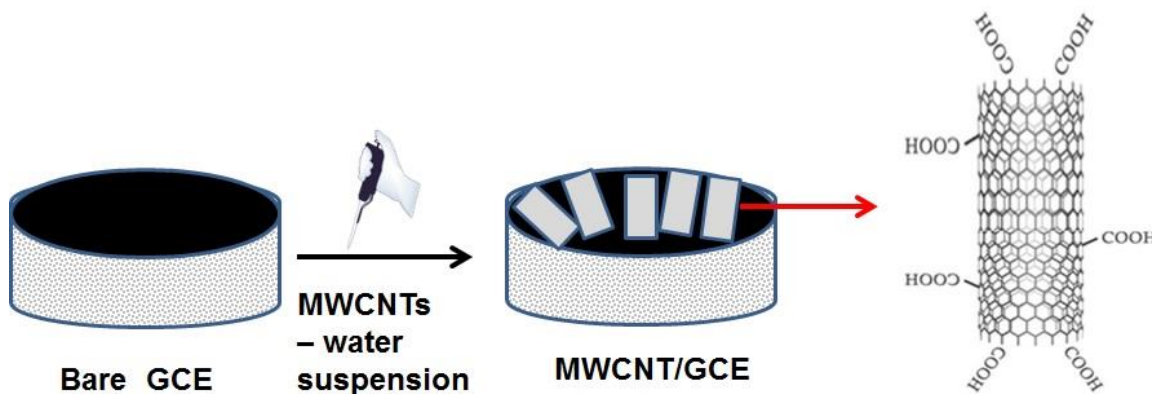
### 2.3. Preparation of carboxylated MWCNT

The commercial MWCNT could not dispersed in water due to the absence of functional group. Hence we functionalize the MWCNT with acid treatment procedure to introduce hydrophilic functional groups. A chemical oxidation treatment of MWCNT [26] was carried out with a mixture of concentrated nitric and sulphuric acids. About 50 mg of was added to 24 mL of the acid mixture in and the mixture was refluxed for 5 h. It is cooled and washed with plenty of double distilled water.

Scheme 1 clearly depicts the carboxylated MWCNT. The acid treated MWCNT could be easily dispersed in aqueous solution by sonication due to the presence of carboxylic acid and hydroxyl groups. The dispersions were quite stable for several weeks and could be stored and reused for several experiments.



**Scheme 1.** Schematic representation of carboxylated MWCNT



Scheme 2. Fabrication of MWCNT/ GCE

#### 2.4. Preparation of Functionalized MWCNT modified glassy carbon electrode (MWCNT/GCE)

1 mg of carboxylated f-MWCNT was dispersed in 1 mL of double water by sonication. 5  $\mu$ L of the dispersion was casted on a polished GCE and then dried in air to obtain MWCNT/GCE. Scheme 2 represents the coating of MWCNT onto the GCE.

### 3. RESULTS AND DISCUSSIONS

#### 3.1. FT-IR Spectrum Characterization

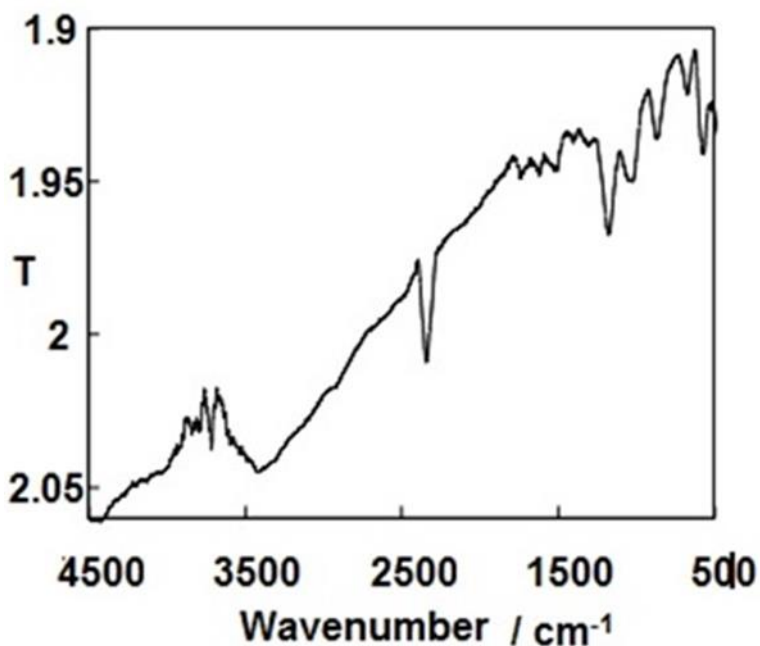
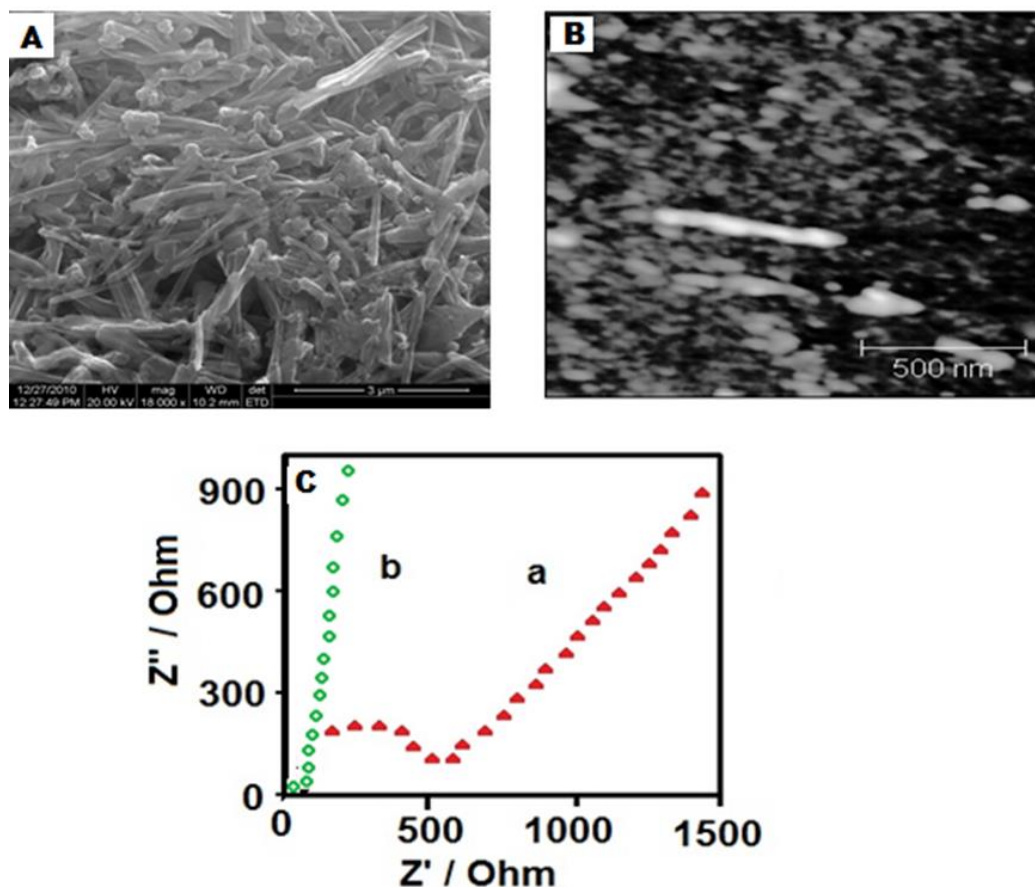


Figure 1. FT IR spectrum of carboxylated MWCNT

The FT-IR spectrum of the commercial sample does not show well defined features and is similar to that of non-functionalized MWCNT [4]. The FT-IR spectrum of functionalized f-MWCNT (Fig. 1) is quite different from that of the commercial sample due to the presence of many new bands. The bands at  $1307\text{ cm}^{-1}$ ,  $1775\text{ cm}^{-1}$ , and  $1405\text{ cm}^{-1}$  correspond to C-O, C-O-C, C=C bonds respectively while the bands at  $1739\text{ cm}^{-1}$  and  $3414\text{ cm}^{-1}$  confirm the presence of functional groups of C=O and -OH respectively [27].

### 3.2. Morphological and Surface Characterization

The morphologies of the functionalized samples of f-MWCNT are obtained by high resolution scanning electron microscopy (HRSEM). The HRSEM image (Fig.2A) of carboxylated MWCNT shows randomly oriented tubular morphology [28]. Unlike the morphology of the commercial sample, carboxylated MWCNTs found to show a rather smooth surface with somewhat closed side-walls. The surface topographical AFM image of carboxylated MWCNT (Fig.2 B) shows the presence of non-uniform tubular structures.



**Figure 2.** (A) HRSEM image of carboxylated f-MWCNT (B) AFM image of functionalized MWCNT (C) Nyquist plot for (a) GCE and (b) f-MWCNT/GCE in 0.1 M KCl containing 1 mM of potassium ferrocyanide solution.

### 3.3 Electrochemical Impedance Spectroscopy (EIS)

EIS is a valuable technique that can be used to investigate the effect of electrode surface modification on the electron transfer process. Fig. 2C shows the results of EIS at bare GCE and MWCNT/GCE in 0.1 M potassium chloride containing 1 mM potassium ferrocyanide in the frequency range between 1 Hz to 1 MHz. At GCE and MWCNT/GCE, a semicircle and a straight line is noted which explains the diffusion controlled Warburg impedance. The diameter of the semicircle refers to the charge transfer resistance ( $R_{ct}$ ) which is found to be nearly 10 times lower at MWCNT/GCE ( $R_{ct} = 47 \Omega$ ) compared to GCE ( $R_{ct} = 496 \Omega$ ). The lower charge transfer resistance can be ascribed to the higher conductivity of MWCNT compared to GCE.

### 3.4 Electrochemical Characterization

The electrochemical characterization of the MWCNT/GCE is carried out in deaerated phosphate buffer solution (pH 6). Fig. 3 shows the cyclic voltammograms of MWCNT/GCE at various sweep rates. A redox couple is observed ( $E_{pa} = -0.188 \text{ V}$ ,  $E_{pc} = -0.35 \text{ V}$  at  $0.02 \text{ V s}^{-1}$ ) in potential range between -0.6 and +0.8 V. The magnitudes of redox peaks are found to vary linearly with sweep rate (Inset in Fig. 3) suggesting the presence of a surface-confined species. A similar electrochemical observation was reported in the literature for MWCNT functionalized using different procedures such as sonochemical [29] and electrochemical oxidation methods [30] and has been attributed to the protonation/deprotonation reaction of the quinone moieties formed during the carboxylation of the MWCNT.

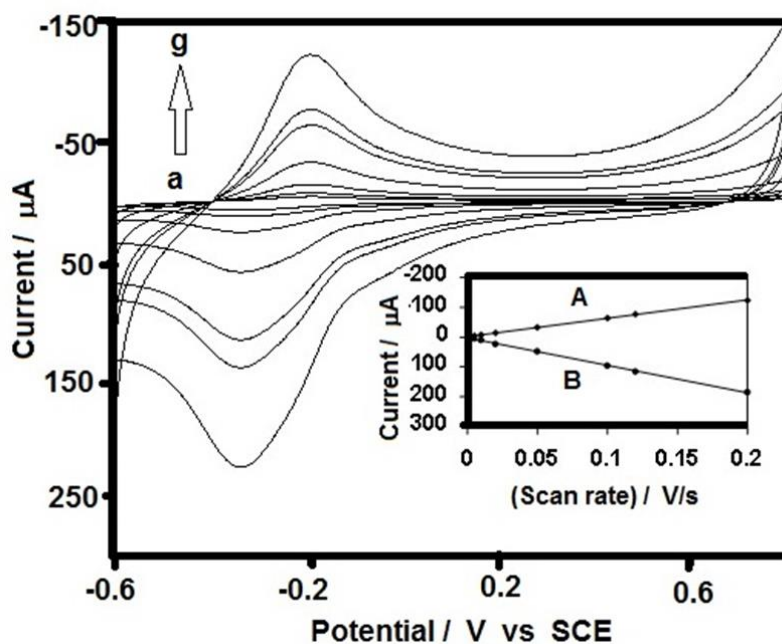


**Figure 3.** Cyclic voltammograms of MWCNT/GCE in 0.1 M PBS (pH 6) buffer solution at various scan rate (a)  $0.005 \text{ V s}^{-1}$  (b)  $0.01 \text{ V s}^{-1}$  (c)  $0.02 \text{ V s}^{-1}$  (d)  $0.05 \text{ V s}^{-1}$  (e)  $0.1 \text{ V s}^{-1}$  (f)  $0.12 \text{ V s}^{-1}$  (g)  $0.2 \text{ V s}^{-1}$ . Inset: Plot of (a) oxidation peak current and (b) reduction peak current vs scan rate.

## 3.5. Cyclic Voltammetric Behavior of Mexacarbate at GCE and MWCNT/GCE – A Comparison

Figs 4 shows the cyclic voltammogram at bare GCE obtained in the potential range of -0.4 V to 1.0 V in deaerated 0.1 M PBS pH 6 containing  $1 \times 10^{-3}$  M mexacarbate at the scan rate of  $0.05 \text{ V s}^{-1}$ . During the first anodic scan, a large oxidation peak at 0.72 V is observed which is irreversible. In the reverse cathodic scan, a small reduction peak at -0.07 V is formed which give rise to a corresponding oxidation peak at -0.01 V in the second anodic scan. Similar observations are made in the cyclic voltammogram at MWCNT/GCE (Fig. 5) which oxidizes at 0.66 V and the redox couple is observed at ( $E_{pa} = 0.11 \text{ V}$ ,  $E_{pc} = -0.07 \text{ V}$ ). The lower oxidation potential of mexacarbate could be attributed to the substituent effect i.e. the presence of an additional electron releasing methyl group in mexacarbate favours the oxidation process.

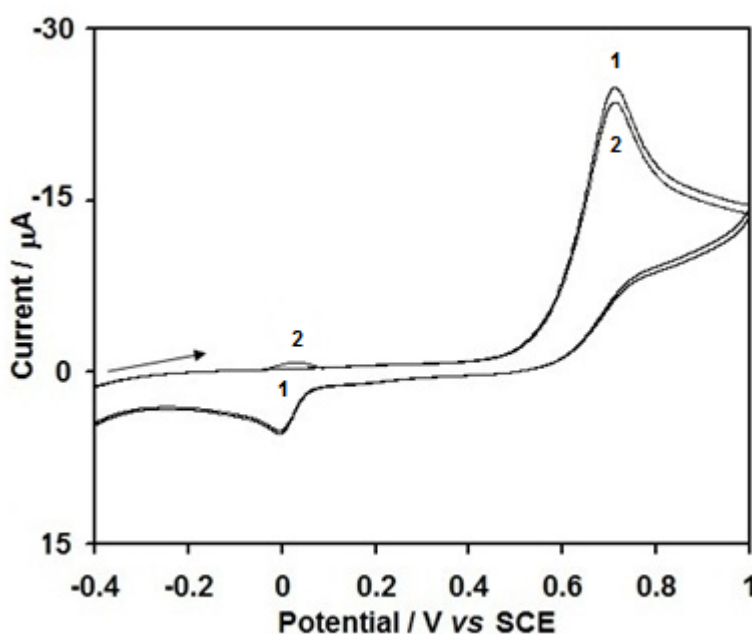
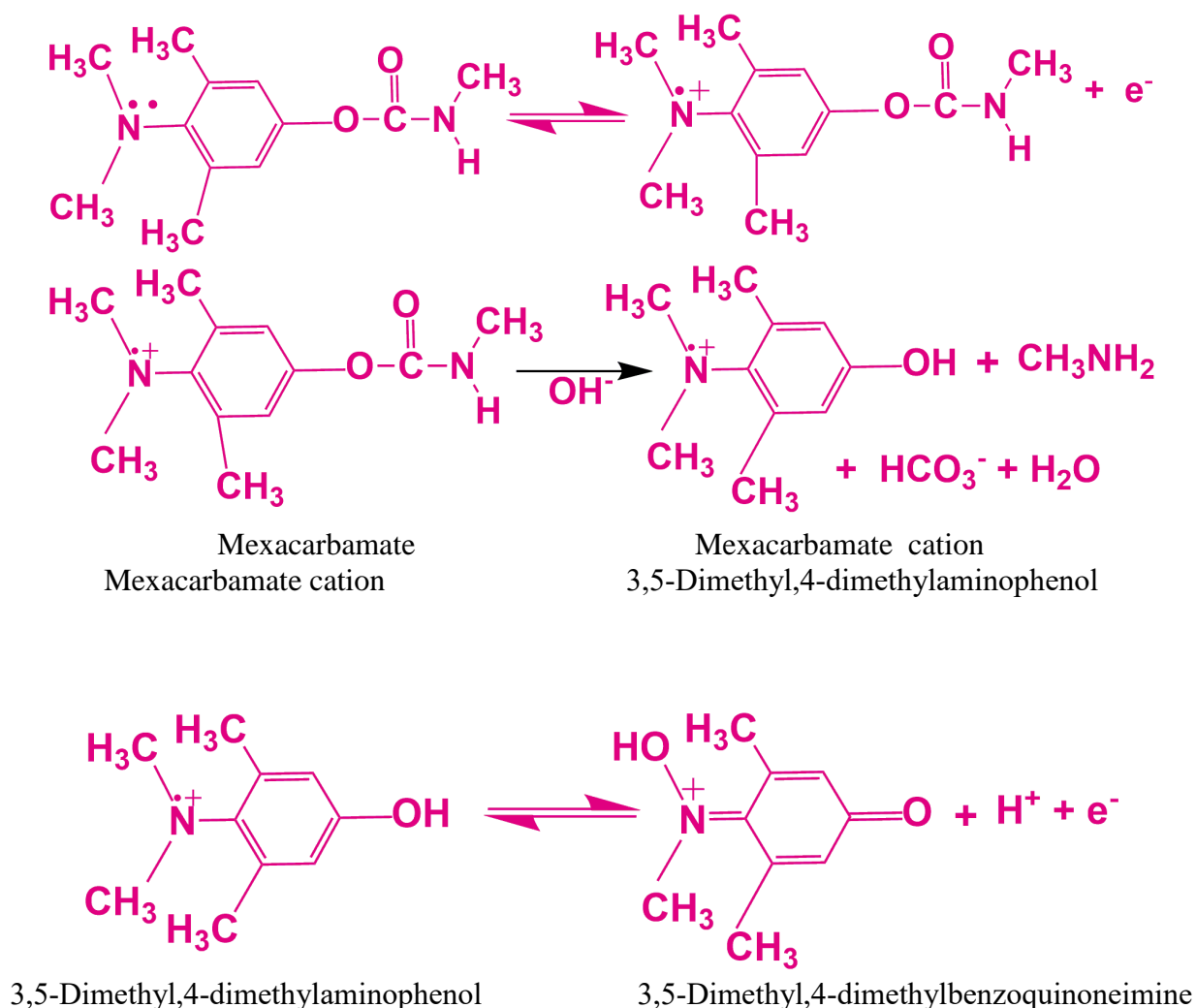


**Figure 4.** Cyclic voltammogram at GCE in 0.1 M PBS (pH 6) buffer solution containing 1mM mexacarbate. Scan rate =  $0.05 \text{ V s}^{-1}$ ; 1 and 2 represent the cycle numbers.

There had been only one report in the literature on the voltammetric analysis of mexacarbate [16]. In that study, it has been shown that the oxidation of mexacarbate involves a ECE reaction (Electron transfer, Chemical reaction, Electron transfer) with a carbamate cation radical as the likely intermediate formed by a one-electron transfer process (Scheme 1). The large anodic peak observed at 0.66 V for mexacarbate in the cyclic voltammograms shown in Figure 5 corresponds to this reaction. The unstable carbamate cation radical undergoes rapid hydrolysis resulting in the formation of 3,5-Dimethyl,4-dimethylaminoethanol radical and methylamine. The phenol derivative then undergoes a second spontaneous oxidation to give 3,5-Dimethyl,4-dimethylbenzoquinoneimine as the product. The redox couple ( $E_{pa} = 0.12 \text{ V}$ ,  $E_{pc} = -0.06 \text{ V}$ ) in the cyclic voltammograms of mexacarbate can be identified with this reaction.



**Scheme 3.** Oxidation reaction of mexacarbamate [5]

The significant observation is that the oxidation potential shifts favorably by 0.16 V for mexacarbamate respectively along with a nearly 1.6 times increase in peak current at MWCNT/GCE compared to bare GCE. This means that the MWCNT/GCE electrocatalysis the oxidation of mexacarbamate and promote the fast one-electron transfer reaction. These results can lead to the micromolar determination of mexacarbamate possible with a better sensitivity. The better performance of electrocatalytic activity of mexacarbamate at MWCNT can be explained as follows.

This is due to the reason of the electrostatic attraction between the positively charged mexacarbamate and the negatively charged carboxylic group at the surface of the multiwalled carbon nanotube. The carboxylic group present in the f-MWCNT acts as the electron acceptor which would decrease the electron density and decrease the electron delocalization of f-MWCNT [31]. Hence, more readily the oxidation of mexacarbamate takes place. F-MWCNT consist of multiple layers of graphite superimposed and rolled to form the tubular shape. Each carbon nanotube held with another carbon nanotube by mean of van der waal forces, each carbon is  $sp^2$  hybridized and contain delocalized  $\Pi$ -electron which is ready to interact with the molecules containing  $\Pi$ -electrons. The structure of

mexacarbate consists of substituted aromatic amine which interacts with the MWNT via  $\Pi$ - $\Pi$  interactions. The higher specific area of f-MWNT contributes to the electrolytic performances of f-MWCNT/GCE. The presence of more capacitive current at MWCNT is due to the presence of the functional group in MWCNT.

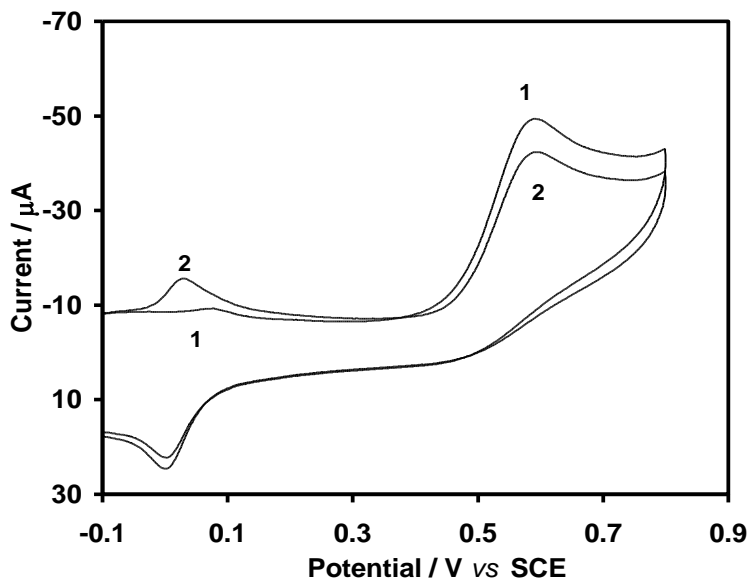


**Figure 5.** Cyclic voltammogram at MWCNT/GCE in 0.1 M PBS (pH 6) buffer solution containing 1mM mexacarbate. Scan rate =  $0.05 \text{ V s}^{-1}$ ; 1 and 2 represent the cycle numbers.

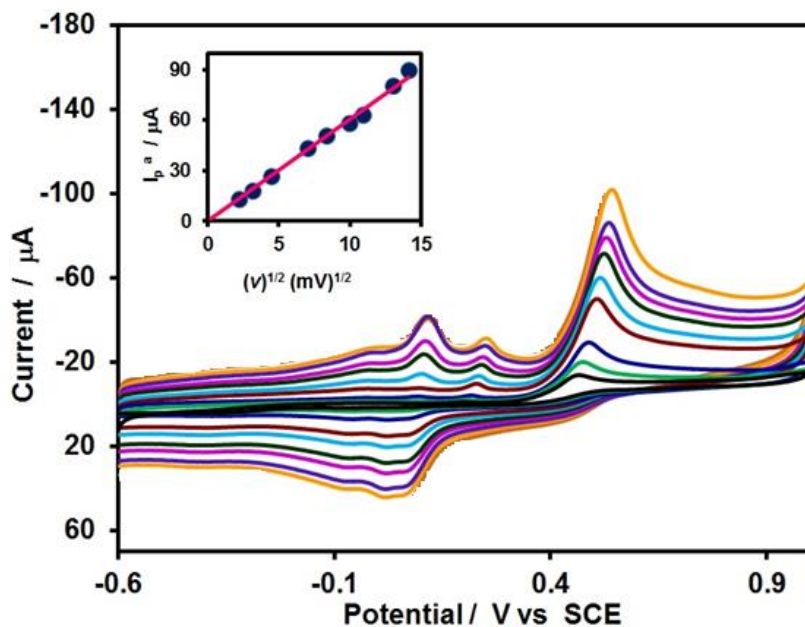


**Figure 6.** Cyclic voltammograms of f-MWCNT/GCE in 0.1 M PBS (pH 6) buffer containing 1mM mexacarbate at various scan rate (a)  $0.005 \text{ V s}^{-1}$  (b)  $0.01 \text{ V s}^{-1}$  (c)  $0.02 \text{ V s}^{-1}$  (d)  $0.05 \text{ V s}^{-1}$  (e)  $0.1 \text{ V s}^{-1}$  (f)  $0.12 \text{ V s}^{-1}$  Inset: Plot of (a) oxidation peak current vs scan rate

Fig 6 show the cyclic voltammogram of mexacarbate at f-MWCNT/GCE in phosphate buffer (pH 6) solution at different scan rate. The insets in this figure show a linear plot of the magnitude of the oxidation peak current against the square root of scan rate suggesting confirming the diffusion-controlled nature of the one-electron oxidation of the mexacarbate to their respective cation radical.

### 3.6. Rotating Disc Electrode (RDE) Measurements

RDE data are obtained at f-WCNT/GCE to confirm the main oxidation of mexacarbate which involves the transfer of one electron through the use of Levich equation [32] (Eq.1)

$$I_L = 0.62 n F A \omega^{1/2} D^{-2/3} \gamma^{-1/6} C \tag{1}$$

where  $I_L$  is the limiting current,  $n$  is the number of electrons transferred,  $F$  is Faraday constant,  $D$  is the diffusion coefficient ( $\text{cm}^2 \text{s}^{-1}$ ) of mexacarbate,  $\gamma$  is the kinematic viscosity ( $\text{cm}^2 \text{s}^{-1}$ ) and  $\omega$  is the angular frequency (rps). The RDE experiments at f-MWCNT/GCE give well-defined current-voltage curves. The Levich plots (magnitude of  $I_L$  vs  $\omega^{1/2}$ ) for the 1mM mexacarbate oxidation at the MWCNT/GCE in the angular frequency values ranging from 2 to 15 rps are shown respectively in Fig.7. The Levich plot shows good linearity for mexacarbate and the number of electrons for the oxidation of mexacarbate is calculated to be nearly 1 assuming a  $D$  value of  $1 \times 10^{-5} \text{ cm}^2 \text{ s}^{-1}$  and  $\gamma$  value of  $1.0 \times 10^{-2} \text{ cm}^2 \text{ s}^{-1}$  [32].

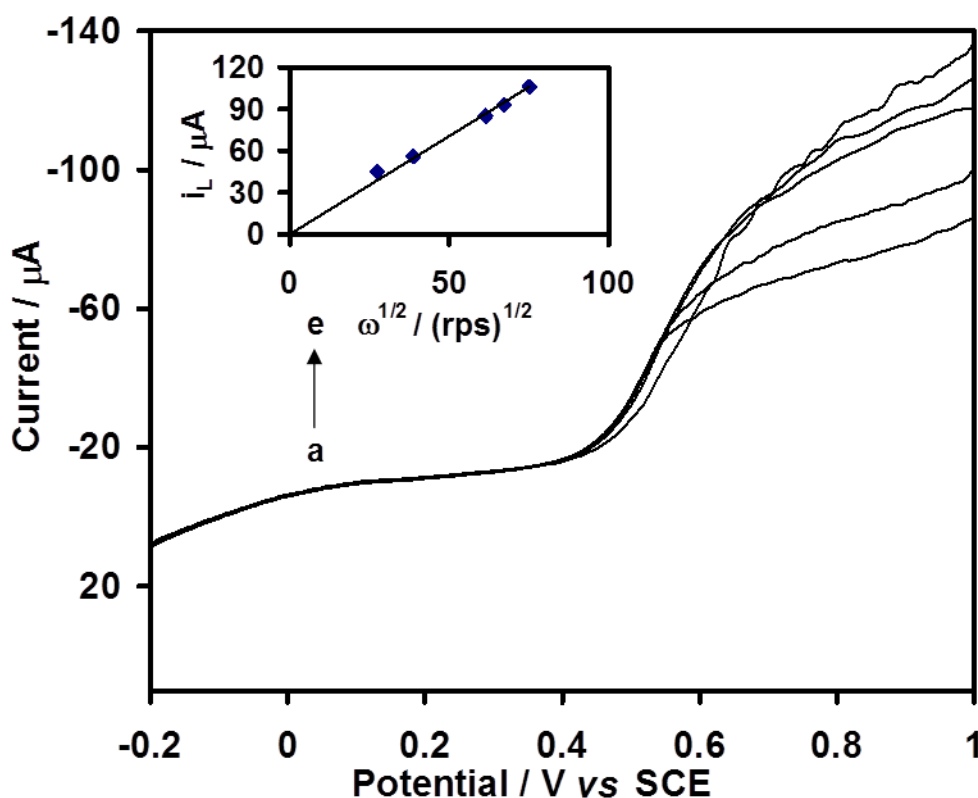
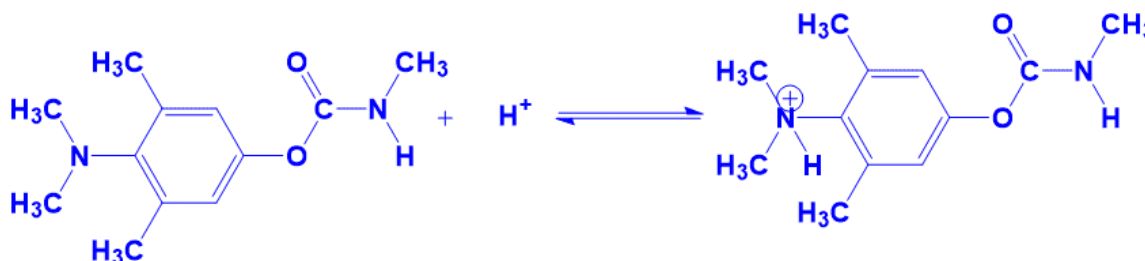


**Figure 7.** RDE of f-MWCNT/GCE in 0.1 M Phosphate buffer solution ( pH 6) containing 1 mM mexacarbate at various rotational speed (a) 2 rps (b) 4 rps (c) 6 rps (d) 8 rps (e) 15 rps. Insert: Plot of anodic peak current versus square root of the rotation speed.

## 3.7. Effect of pH

Mexacarbamate could be protonated as shown in Scheme 2 which may affect the electrochemical oxidation reaction. Therefore, it becomes pertinent to study the influence of hydrogen ion concentration. Also, it is essential to obtain the optimum pH value for observing maximum sensitivity in the sensing of the mexacarbamate.



**Scheme 4.** Protonation of the dimethyl amino group in mexacarbamate

Therefore, the cyclic voltammograms at f-MWCNT/GCE are recorded at  $0.05 \text{ V s}^{-1}$  in 0.1 M acetate buffer (pH 3, 4, 5) and 0.1 M PBS (pH 6, 7 and 8). Fig. 8 shows the plot of the oxidation peak current and peak potential versus pH for  $1 \times 10^{-3} \text{ M}$  mexacarbamate. From these data, it is inferred that the highest current is observed in 0.1 M phosphate buffer (pH 6). Therefore, further calibration experiments have been carried out in this electrolyte.

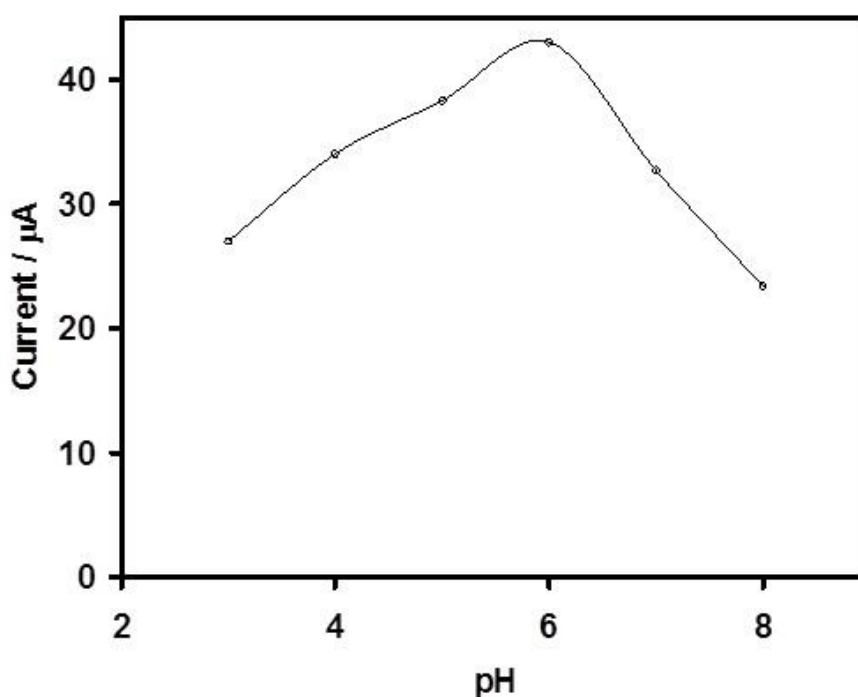


**Figure 8.** Plot of oxidation peak current vs pH in  $1 \times 10^{-3} \text{ M}$  of mexacarbamate. Scan rate =  $0.05 \text{ V s}^{-1}$

### 3.8. Differential Pulse Voltammetry

Differential pulse voltammetry (DPV) is an useful analytical technique for measuring the trace levels of inorganic species and organic species [33]. DPV experiments have been performed at f-MWCNT/GCE in the potential range from 0.3 to 0.7 V using the following optimal parameters: scan increment 0.004 V and pulse amplitude of 0.05 V in PBS (pH 6). Figs. 9 show the DPVs in the concentration range between  $1.5 \times 10^{-5}$  M to  $2 \times 10^{-7}$  M and insert shows the sensor calibration plot for mexacarbate. The current response is found to be linear in the entire concentration range giving the slope and regression coefficient values of  $0.15 \mu\text{A} / \mu\text{M}$  and 0.98, respectively for mexacarbate.

The detection limit can be calculated using Eq. 2

$$\text{Detection Limit} = \frac{3 \times S_b}{N} \quad (2)$$

where N is the slope of the calibration curve and  $S_b$  is the standard deviation of blank solution. The signal-to-noise ratio is the ratio between the mean value of the repeat measurements at the lowest concentration used and its standard deviation. In this study, the standard deviation for mexacarbate is calculated to be 0.0610. The detection limit for mexacarbate is calculated to be  $1.54 \times 10^{-8}$  M. The detection limit observed in the present study is compared with that reported in the literature for bare glassy carbon electrode.

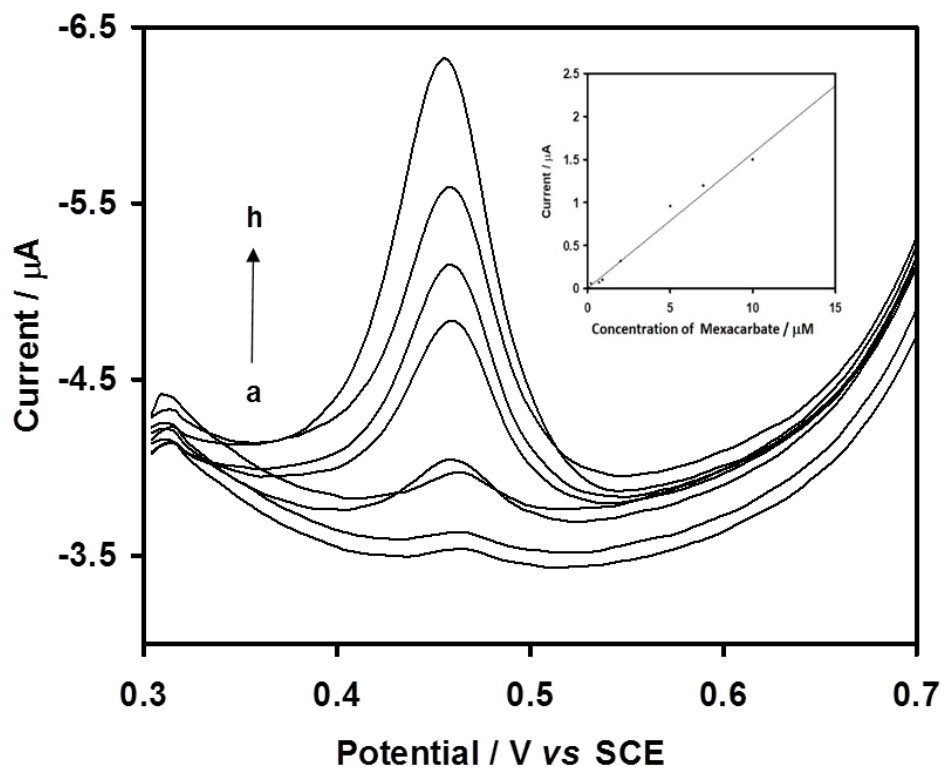


**Figure 9.** Differential pulse voltammograms at f-MWCNT/GCE in 0.1M PBS (pH = 6) at different concentrations of mexacarbate (a)  $2 \times 10^{-7}$  M (b)  $7 \times 10^{-7}$  M (c)  $9 \times 10^{-7}$  M (d)  $2 \times 10^{-6}$  M (e)  $5 \times 10^{-6}$  M (f)  $7 \times 10^{-6}$  M (g)  $1 \times 10^{-5}$  M and (h)  $1.5 \times 10^{-5}$  M Insert: Calibration plot for mexacarbate sensor.

### 3.9. Real sample analysis

In order to prove the feasibility of the f-MWNT/GCE, the proposed method was applied for determining mexacarbate in water sample. The water samples were spiked with a mexacarbate concentration of mexacarbate of 8  $\mu\text{M}$  and 7  $\mu\text{M}$ . The two samples were measured by DPV in 0.1 M PBS (pH 6). Table 1 show the recovery percentage of mexacarbate range from 85 %- 87% with relative standard deviation of 3% to 5%. Those results confirms the practical application of mexacarbate in the water samples. Table 2 shows literature survey for sensing of mexacarbate by different analytical methods [35, 36]. The limit of detection obtained DPV is comparable with reversed-phase high-performance liquid chromatography coupled with electrospray ionisation mass spectrometry and electrospray ionization–mass spectrometry

**Table 1.** A recovery study of mexacarbate present in water at MWCNT/GCE.

Sample	Added ( $\mu\text{M}$ )	Found ( $\mu\text{M}$ )	Recovery %
Water	8	7.0	85
Water	7	6.2	89

**Table 2.** Reported limit of detection data for mexacarbate sensor using different analytical method

Type of Materials	Method	Detection Limit (mM)	Ref
GCE	DPV	0.135	16
SPE C-18 cartridges	RP-HPLC coupled to ESI	0.004	35
MWCNT	ESI– MS	0.00197	36
GCE/MWCNT	DPV	0.0154	Present work

RP-HPLC - Reversed-phase high-performance liquid chromatography

ESI - Electrospray ionisation mass spectrometry

SPC C18- Solid phase extraction cartridges 18

ESI– MS- Electrospray ionization–mass spectrometry

## 4. CONCLUSION

The commercial multi-walled nanotube (MWCNT) has been carboxylated and characterized by various techniques. Carboxylated multi-walled carbon nanotube exhibits the catalytic activity for the sensing of mexacarbate. A comparison of the cyclic voltammetric behavior at glassy carbon electrode

(GCE) and MWCNT/GCE suggests that the oxidation potential shifts favorably by 0.16 V for mexacarbate along with the nearly 1.6 times increase in anodic peak current at MWCNT/GCE compared to bare GCE. The MWCNT/GCE shows good stability, reproductively and towards mexacarbate.

#### ACKNOWLEDGEMENTS

This project was supported by King Saud University, Deanship of Scientific Research, College of Science, Research Center. The authors are grateful for financial support (MOST 107-2113-M-027-005-MY3) from the Ministry of Science and Technology (MOST) and Ministry of Education, Taiwan.

#### References

1. J.H.A. Ruzicka, Organophosphorus and carbamate detection system, *Pest Management Science* 4 (1973) 417
2. P. Qi, J. Wang, X. Wang, Z. Wang, H. Xu, S. Di, Q. Wang and X. Wang, *RSC Adv* 8(2018) 25334
3. N. Kokot, Q. Serge, Yongnian and Ping, *Anal. Chim. Acta* 321 (2005) 537.
4. T.N. Rao, B.H. Loo, B.V. Sarada, C. Terashima, and A. Fujishima, *Anal. Chem* 74(2002) 1578
5. J.M. Sorian, B. Jiménez, G. Font, and Moltó. *Crit. Rev. Anal. Chem.* 19(2001) 31
6. Y. Li, R. Zhao, L. Shi, G. Han and Y. Xiao, *RSC Adv.*, 7 (2017) 53570
7. A.D. Corcia, R. Samperi, A. Marcomini, and S. Stelluto, *Anal. Chem* 65 (1993) 907
8. H.S. Rathore, and T. Begum, *J. Chromatogr. A* 321 (1993) 643
9. A.L. Howard, C. Braue, and L.T. Taylor. *J. Chromatogr. Sci.* 31 (1993) 323.
10. S.S. Yang, and A.I. Goldsmith, *J. Chromatogr. A* 3 (1996) 754.
11. G. C. Mattern, G.M. Singer, J. Louis, M. Robson, and J.D. Rosen, *J. Agri. Food. Chem.* 38 (1990) 402.
12. H. Faerber, and H.F. Schoeler, *J. Agri. Food. Chem.* 41(1993) 217.
13. L.F.C. Vallvey, J. Rohand, A. Navalón, R. Avidad, and J.L. Vilchez, *Talanta* 40 (1993) 1695.
14. A. Guiberteau, T.G. Diaz, F. Salinas, and J. M. Ortiz, *Anal. Chim. Acta* 219 (1995) 305
15. Y. Ni, P. Qiu, and S. Keket, *Anal. Chim. Acta* 321 (2005) 537.
16. G. E. Batley, and B.K. Afgan, *J. Electroanal. Chem.* 125 (1981) 437.
17. T.M.G. Selva, W.R. Araujo, R.P. Bacil, and T.R. L.C. Paixão, *Electro. Chim. Acta*, 246 (2017) 588.
18. D.J.E. Costa, J.C.S. Santos, F.A.C.S. Brandão, W.F. Ribeiro, G.R.S. Banda, and M. C. U. Araujo, *M. J. Electroanal. Chem.* 100 (2017) 789.
19. J. Chýlková, M. Tomášková, I. Švancara, L. Janíková, and R. Šelešovská, *Anal. Methods.* 7 (2015) 4671
20. T.N. Rao, B.H. Loo, B.V. Sarada, C. Terashima, and A. Fujishima, *Anal. Chem.* 74 (2002) 1578.
21. S.R. Belding, F.W. Campbell, E.J.F. Dickinson, and R.G. Compton, *Phys. Chem. Chem. Phys.* 2012, vol. 12, p. 11208.
22. I. Tonle, and E. Ngameni (Ed.), Intech, Croatia, 2011
23. N. Kaur, N. Prabhakar, *Trends. Anal. Chem.* 2017, 62 (2017) 92.
24. M.T.F. Abedul, and A.C. García, *Anal. Bioanal. Chemistry* 390 (2008) 293
25. C. Hu, and H. Shengshui, *J. Sensors* 40 (2009) 187615.
26. M.S.P. Shaffer, X. Fan and A.H. Whindle, *Carbon*, 36 (1998) 1603
27. V.T. Le, C.L. Ngo, Q.T. Le, T.T. Ngo, and D.N. Nguyen, *Adv. Nat. Sci. Nanosci. Nanotechnol.* 1 (2013) 4
28. S. Suresh, A.K. Gupta, V.K. Rao, O. Kumar and R. Vijayaraghavan, *Talanta*, 81(2010) 703.
29. H. Zhang, X. Wang, L. Wan, Y. Liu, and C. Bai, *Electrochim. Acta* 49 (2004) 715.

30. H. Zheng, L. Lin, Y. Okezaki, R.K. Akami, H. Sakuraba, T. Ohshima, K. Takagi, and S.I.Suye, *Beilstein J. Nanotechnol.* 1( 2010) 135.
31. Y. Sang, B. Wang, Q. Wang, G. Zhao, and P. Guo, *Scientific Reports* 1(2014) 4.
32. Y.Li, R. Lenigk, X.Wu, B.Gruendig, S. Dong, and R. R. Renneberg, *Electroanal* 10 (1998) 671
33. Bard, A. J., and Faulkner, L R., 2001. *Electrochemical Methods: Fundamentals and Applications*, John Wiley, New York
35. F. Boujelbane, F. Oueslati, N. Ben Hamida, *Desalination* 250 (2010) 473
36. L. Latrous E. Atrache, M. Hachani, B. B. Kefi , *Int. J. Environ. Sci. Technol.* 13 (2016) 201

© 2019 The Authors. Published by ESG ([www.electrochemsci.org](http://www.electrochemsci.org)). This article is an open access article distributed under the terms and conditions of the Creative Commons Attribution license (<http://creativecommons.org/licenses/by/4.0/>).